

Magnetic mesoporous carbon material with strong ciprofloxacin adsorption removal property fabricated through the calcination of mixed valence Fe based metal-organic framework

Chunyu Jiang¹ · Xiaoxing Zhang¹ · Xinxin Xu¹ · Linshan Wang¹

Published online: 26 April 2016
© Springer Science+Business Media New York 2016

Abstract As an efficient and low cost adsorbent to remove fluoroquinolones antibiotics (such as ciprofloxacin and norfloxacin) in waste water, magnetic mesoporous carbon material has attracted increasing concern all over the world. Here, a convenient strategy to fabricate magnetic mesoporous carbon material has been explored with Fe containing metal-organic framework (MOF) as precursor. With this method, a magnetic mesoporous carbon material, Fe₃O₄/C, which possesses high surface area, is obtained through the calcination of a mixed valence Fe based MOF. For Fe₃O₄/C, its ciprofloxacin adsorption capacity reaches as high as 868.6 mg/g. Magnetic measurement reveals its ferromagnetic feature of Fe₃O₄/C with magnetization saturation 22.81 emu g⁻¹ and this guarantees its excellent magnetic separation performance. Furthermore, Fe₃O₄/C also exhibits outstanding stability during ciprofloxacin containing waste water treatment.

Keywords Mesoporous carbon · Fe₃O₄ · Composite material · Ciprofloxacin adsorption

1 Introduction

Ciprofloxacin, the third generation of fluoroquinolones, is a widely used antibiotic all over the world [1]. As other antibiotics, ciprofloxacin cannot be fully metabolized in body and the rest part is excreted directly [2]. Now its presence in aquatic environment has led to serious bacterial drug resistance in human being, which poses serious threat to us [3, 4]. For its low energy consumption and high efficiency characteristics, adsorption has been proven to be one of the most effective and simplest approaches that have been employed for antibiotic containing waste water treatment [5]. In the family of adsorbents, mesoporous carbon material are more attractive than other members due to its uniform pore architecture, high surface area, large pore volume and excellent chemical stability [6]. Although these features make mesoporous carbon material becomes a promising adsorbent, unavoidably problem still appears as it is employed in practical ciprofloxacin polluted water disposal, because of the difficulty in separation from the treated waste water [7].

Magnetic materials, especially Fe₃O₄ can solve this problem successfully with unique magnetic separation technology, which has been proved to be powerful approach for the separation and purification [8, 9]. With this method, Fe₃O₄ is used as a “building block” to assemble with mesoporous carbon and construct a composite material [10]. In resulted composite material, ferromagnetic property of Fe₃O₄ allow its easy separation and recovery from waste water by the application of an external magnetic field [11]. But as a sensitive material, ferromagnetic property of Fe₃O₄ will invalid under acidic or oxidative condition [12]. To protect susceptible Fe₃O₄ from erosion in ciprofloxacin containing waste water, the only approach is embedding it in mesoporous carbon.

Electronic supplementary material The online version of this article (doi:10.1007/s10934-016-0188-x) contains supplementary material, which is available to authorized users.

✉ Xinxin Xu
xuxx@mail.neu.edu.cn

✉ Linshan Wang
lswang@mail.neu.edu.cn

¹ Department of Chemistry, College of Science, Northeast University, Shenyang 110819, Liaoning, People’s Republic of China

To achieve this purpose, we fall back on metal-organic framework (MOF), a kind of porous crystalline material constructed from metal ion and organic ligand, which has been used as precursors to prepare mesoporous carbon material very recently [13–20]. Here, a composite material constructed from Fe_3O_4 and mesoporous carbon (named as $\text{Fe}_3\text{O}_4/\text{C}$) was synthesized successfully through the carbonization a mixed valence Fe-based metal organic framework, MIL-53(Fe(III)/Fe(II)). In the structure of $\text{Fe}_3\text{O}_4/\text{C}$, Fe_3O_4 with the dimension about 30–40 nm is embedded in mesoporous carbon. $\text{Fe}_3\text{O}_4/\text{C}$ composite material possesses excellent ferromagnetic character with magnetization saturation 22.81 emu/g at room temperature, which is enough for magnetic separation. At the same time, it also possesses high surface area and excellent ciprofloxacin adsorption property. Furthermore, the adsorption and magnetic properties are well retained after five cycles ciprofloxacin adsorption and desorption treatments.

2 Experimental

2.1 Materials and synthesis

All purchased chemicals were of reagent grade and used without further purification. PXRD patterns were recorded on D8 X-ray diffractometer, employing monochromatized $\text{CuK}\alpha$ incident radiation. The X-ray photoelectron spectroscopy (XPS) measurements were carried out on a Thermo Scientific ESCALAB 250 instrument with a monochromatic $\text{AlK}\alpha$ source. The morphology was observed on an ultra plus field emission scanning electron microscope (FESEM; ZEISS, Germany) and transmission electron microscopy (TEM; FEI Tecnai G2 F20) operated at 200 kV. Thermogravimetric analyses were performed on a Perkin-Elmer TGA7 instrument in flowing N_2 with a heating rate of 10 °C/min. Nitrogen adsorption/desorption isotherms were measured using a Micromeritics ASAP 2020 M volumetric gas sorption instrument and 99.999 % pure N_2 . The magnetization curve was measured at room temperature under varying magnetic field from -8.0 to $+8.0$ KOe on a BHV-55 vibrating sample magnetometer. Agilent 1200 HPLC was used to analyze the equilibrium concentration of ciprofloxacin.

2.2 Synthesis of MIL-53 (Fe(III))

MIL-53(Fe(III)) was prepared according to Férey's methods with some expansion [21]. In a typical synthesis, $\text{FeCl}_3 \cdot 6\text{H}_2\text{O}$ (0.068 g, 0.25 mmol), terephthalic acid (BDC) (0.083 g, 0.5 mmol) were dissolved in 8 mL dimethylformamide (DMF). The mixture was stirred for 20 min and then transferred to a 15 mL Teflon-lined stainless steel bomb and kept at 180 °C under autogenously

pressure for 72 h. The reaction system was cooled to room temperature during 24 h. A large amount of small yellow crystals were found.

The crystals were grinded for 3 h with an agatemortar and pestle. The resulted powder was dissolved in methanol and placed in a Teflon autoclave, which was heated in a microwave oven at 200 W for 2 h. The resulted MIL-53(Fe(III)) was separated by centrifugation, rinsed with water and then dried in a vacuum drier at 120 °C for 24 h.

2.3 Synthesis of MIL-53 (Fe(III)/Fe(II))

At first, MIL-53(Fe(III)) was heated at 150 °C overnight. The resulted solid (0.20 g) was dissolved in 40 mL water. $\text{FeCl}_2 \cdot 4\text{H}_2\text{O}$ (1.2 g $\text{FeCl}_2 \cdot 4\text{H}_2\text{O}$ in 20 mL) was dropped into above solution. The mixture was stirred 48 h to ensure the adequately substitution of FeCl_2 in MIL-53(Fe(III)), and then separated and dried in a vacuum drier at 120 °C for 12 h.

2.4 Synthesis of $\text{Fe}_3\text{O}_4/\text{C}$

The dry powder of MIL-53(Fe(III)) was placed in a tube furnace under N_2 gas flow (1 L/min), heated to 500 °C (2 °C/min), and maintained at this temperature for 3 h. The obtained powder was $\text{Fe}_3\text{O}_4/\text{C}$ composite material.

2.5 Isothermal adsorption

The pH of ciprofloxacin solution was controlled by Britton–Robinson (B–R) buffer within a range of pH 4.78–8.95 (a mixture of 0.04 mol/L phosphoric acid, acetic acid, boric acid, and 0.2 mol/L sodium hydroxide). 10 mg $\text{Fe}_3\text{O}_4/\text{C}$ was added in ciprofloxacin (10 mL, 10–900 mg/L). The mixture was stirred for 2 h at 288 K to reach equilibrium and separated by centrifuging at 4000 rpm for 4 min. The adsorption capacity q_e (mg/g) was calculated by Eq. (1), in which C_0 and C_e represents the initial and equilibrium concentration of ciprofloxacin (mg/L), while V and m are the volume of ciprofloxacin solution and mass of $\text{Fe}_3\text{O}_4/\text{C}$ respectively. To analyze the isothermal data, Langmuir model, Freundlich model and Temkin model were employed from Eqs. (2) to (4). In Eq. (2), K_L and q_m are Langmuir constant and maximum adsorption capacity. In Eq. (3), K_f and n represents Freundlich constant and linearity index. In Eq. (4), R and T are universal gas constant and absolute temperature respectively, while K_T and b_T are Temkin constants.

$$q_e = (C_0 - C_e)V/m \quad (1)$$

$$C_e/q_e = 1/bq_m + C_e/b \quad (2)$$

$$\ln q_e = \ln K_f + 1/n \ln C_e \quad (3)$$

$$q_e = RT/b_T \ln K_T C_e \tag{4}$$

The equilibrium concentration of ciprofloxacin was analyzed by Agilent 1200 HPLC under the following conditions, a Phenomenex Gemini C18 column, 250 mm × 4.6 mm was used for chromatographic separations at 30 °C. The mobile phase, mixed solution of acetonitrile and phosphoric acid (20:80, v/v) containing 2.5 mM 1-heptanesulphonic acid sodium salt, was vacuum filtered with a Water Associates (Milford, MA, USA) filtering kit, w is 0.45 mm. The mobile phase was set at 1.0 mL min⁻¹, the detection wavelength was set at 278 nm.

2.6 Kinetic adsorption study

The adsorption experiments of ciprofloxacin were conducted at different initial concentrations of 400, 600 and 800 mg/L. The dosages of adsorbent, volume of ciprofloxacin and adsorption temperature are similar with isothermal adsorption studies. The mixture of Fe₃O₄/C and ciprofloxacin solution was stirred for certain time and centrifuged to collect the supernatant and determine the concentration of ciprofloxacin. Three adsorption kinetic models, pseudo-first-order model (5) pseudo-second-order model (6) and intra-particle diffusion model (7) were applied to analyze the results. In Eq. (5), k₁ (min⁻¹) is the pseudo-first-order rate constant and q_t is the amount of ciprofloxacin adsorbed at the time t. In Eq. (6), k₂ (mg/g/min) is the pseudo-second-order rate constant and q_t is the amount of ciprofloxacin adsorbed at the time t. In Eq. (7), k₃ (mg/g/ min^{1/2}) is the intra-particle diffusion rate constant and C (mg/g) is a constant represents the thickness of the boundary layer.

$$\ln(q_e - q_t) = \ln q_e - k_1 t \tag{5}$$

$$t/q_t = 1/k_2 q_e^2 + 1/q_e \tag{6}$$

$$q_t = k_3 t^{1/2} + C \tag{7}$$

2.7 Adsorption thermodynamics

To investigate the thermodynamics, 10 mg Fe₃O₄/C was mixed with 10 mL ciprofloxacin (20, 50, 100, 200 and 400 mg/L) and the mixture was stirred at different temperatures (288, 303 and 318 K) for 2 h. The thermodynamic equilibrium constant K for the adsorption was obtained with the method of Raji and Anirudhan [22]. The standard free energy change ΔG was obtained from the following Eq. (8), in which R is the universal gas constant and T is the absolute temperature. The enthalpy change ΔH and entropy change ΔS were calculated by Eq. (9).

$$\Delta G = -RT \ln K \tag{8}$$

$$\ln K = -\Delta H/RT + \Delta S/R \tag{9}$$

2.8 Recovery and desorption property study

After desorption, Fe₃O₄/C was separated with magnetic separation technology with an external magnetic field while mesoporous carbon was separated through centrifugation. Desorption experiments were conducted by mixing Fe₃O₄/C with 5 mL ethanol (10 %). The mixed solution was stirred for 30 min. Then the same procedure was carried out as mentioned above. The remaining solution was analyzed to determine the protein concentration (C₂). The desorption percent (Des, %) was calculated by using Eq. (10):

$$\text{Des\%} = C_2 / (C_0 - C_1) \times 100\% \tag{10}$$

3 Results and discussion

3.1 Structural study of MIL-53(Fe(III)/Fe(II)) and Fe₃O₄/C

At first, PXRD was used to study the structures of MIL-53(Fe(III)) and MIL-53(Fe(III)/Fe(II)), which took on approximately similar diffraction patterns with Férey's report [23]. This implies in MIL-53(Fe(III)), although a part of Fe(III) is substituted by Fe(II), its structure is retained and crystalline nature is not destroyed (Fig. S1). It is also noticed, compared with MIL-53(Fe(III)), the peaks of MIL-53(Fe(III)/Fe(II)) shift to higher degree region. This implies that Fe(II) is doped into the crystal lattice of MIL-53(Fe(III)), because the ionic radius of Fe(II) (0.72 Å) is remarkably larger than Fe(III) (0.64 Å).

PXRD was used to study the structure of the composite material. It can be observed strong peaks appear at 30.3°, 35.5°, 43.1°, 53.5°, 57.3° and 62.5°, which is in accordance with (220), (311), (400), (422), (511) and (440) planes of magnetite Fe₃O₄ respectively (Fig. 1) [24]. But this is insufficient to confirm the existence of Fe₃O₄, since Fe₂O₃ possesses the same PXRD patterns with Fe₃O₄. Furthermore, the diffractions belonging to carbon were disappear and the reason maybe its amorphous form. To illustrate the existence of Fe₃O₄ and carbon in the composite materials, XPS was employed. Survey spectrum of the composite material shows two strong peaks centered at 284.1 and 532.2 eV, which can be ascribed to C 1s and O 1s respectively (Fig. 2a) [25]. The existence of Fe was studied with high-resolution spectrum. The binding energy of Fe appear at 711.3 and 725.2 eV, which correspond to Fe 2p_{3/2} and Fe 2p_{1/2}, which is in agreement with the pattern of Fe₃O₄ (Fig. 2b) [26]. These results can identify the existence of Fe₃O₄ in the composite material.

Morphology of Fe₃O₄/C and MIL-53 (Fe(III)/Fe(II)) were studied with SEM. For MIL-53 (Fe(III)/Fe(II)), the

dimension vary from 2 to 5 μm (Fig. 3a). After pyrolysis, the morphology of MIL-53 (Fe(III)/Fe(II)) is well retained in $\text{Fe}_3\text{O}_4/\text{C}$ (Fig. 3b). TEM shows Fe_3O_4 nanoparticle with the diameter about 40–60 nm dispersed uniformly in the $\text{Fe}_3\text{O}_4/\text{C}$ (Fig. 3c) [27, 28]. For $\text{Fe}_3\text{O}_4/\text{C}$, to analysis its content of Fe_3O_4 and C, thermogravimetric analysis (TGA) was carried out. There exists only one obvious weight loss about 51.8 % as temperature is over 385 $^\circ\text{C}$, which can be attributed to the oxidation of carbon (Fig. 3d). So we can conclude the mass percentage of carbon is estimated to be 51.8 %.

3.2 Adsorption and magnetic properties study

Nitrogen adsorption–desorption isotherms were measured to evaluate the surface area, pore size distribution and pore volume of $\text{Fe}_3\text{O}_4/\text{C}$. The curve shows Type-II BET isotherm, with hysteresis loops between the adsorption and desorption branches, demonstrating the existence of mesopore (Fig. 4a). This composite material shows higher surface area of $908.21 \text{ m}^2 \text{ g}^{-1}$ with pore volume of $0.83 \text{ cm}^3 \text{ g}^{-1}$. Pore size distribution calculated from the adsorption branch illustrates the majority of pores are located in the region of mesopores with a peak centering at

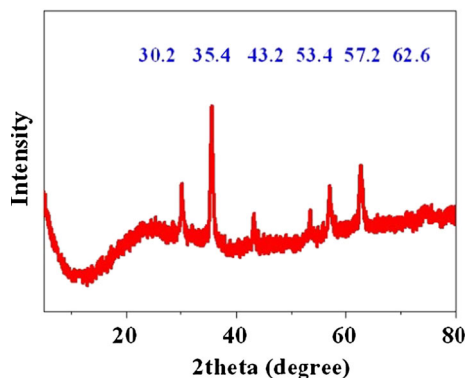
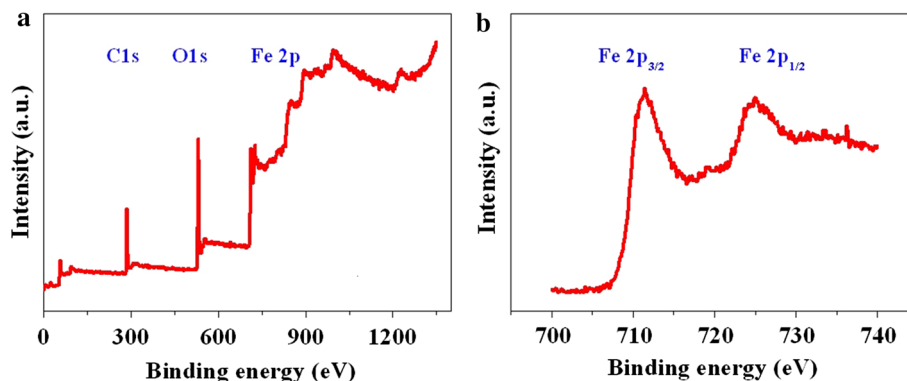


Fig. 1 PXRD of the composite material

Fig. 2 **a** XPS survey of the composite material **b** $\text{Fe } 2p_{3/2}$ and $\text{Fe } 2p_{1/2}$ of the composite material



2.38 nm (Fig. 4b). This dimension is wide enough for the incorporation of ciprofloxacin in the pore. The magnetic measurement was carried out to research the magnetic property of $\text{Fe}_3\text{O}_4/\text{C}$. The field-dependent magnetization curve was conducted between $\pm 8 \text{ KOe}$ and all the curves show a hysteresis loop (Fig. 4c, d) [29]. This implies ferromagnetic feature of $\text{Fe}_3\text{O}_4/\text{C}$ and the saturation magnetization value is 22.81 emu g^{-1} , which is enough for its application in magnetic separation.

3.3 Adsorption isotherm

To study the influence of pH value on adsorption efficiency, the adsorption efficiency of $\text{Fe}_3\text{O}_4/\text{C}$ was investigated within pH 4.78–8.95 (Fig. S1). The results illustrated pH value does not exhibit great influence on adsorption efficiency and this can be attributed to the neutral framework of $\text{Fe}_3\text{O}_4/\text{C}$. Then, adsorption isotherm was applied to analyze the distribution of ciprofloxacin between adsorbent and solution after the system equilibrium is reached at pH 6.80. The results illustrated that ciprofloxacin was adsorbed on surface of $\text{Fe}_3\text{O}_4/\text{C}$ successfully. Adsorption isotherm for ciprofloxacin with $\text{Fe}_3\text{O}_4/\text{C}$ represents the equilibrium concentrations after the adsorption. From adsorption isotherm, we can observe adsorption capacity increases with the addition of ciprofloxacin, but the slopes of adsorption isotherms decrease gradually. When initial concentration is lower than 600 mg/L, the removal efficiency is higher than 93.9 %, but if the initial concentration is higher than this concentration, the removal efficiency falls obviously and achieve 86.8 % at 1000 mg/L (Fig. 5a). In addition, three classic adsorption models, including Langmuir model, Freundlich model and Temkin model, were used to study the adsorption equilibrium. Langmuir model was used to fit the experimental data at first and a high determination coefficient ($R^2 = 0.9975$) is obtain (Fig. 5b). Furthermore, the adsorption capacity calculated based on this model is 843.9 mg/g, which is very close to the experimental value, 868.6 mg/g. This illustrates Langmuir model can describe

Fig. 3 **a** SEM of MIL-53(Fe(III)/Fe(II)) **b** SEM of Fe₃O₄/C **c** TEM of Fe₃O₄/C **d** TGA curve of Fe₃O₄/C

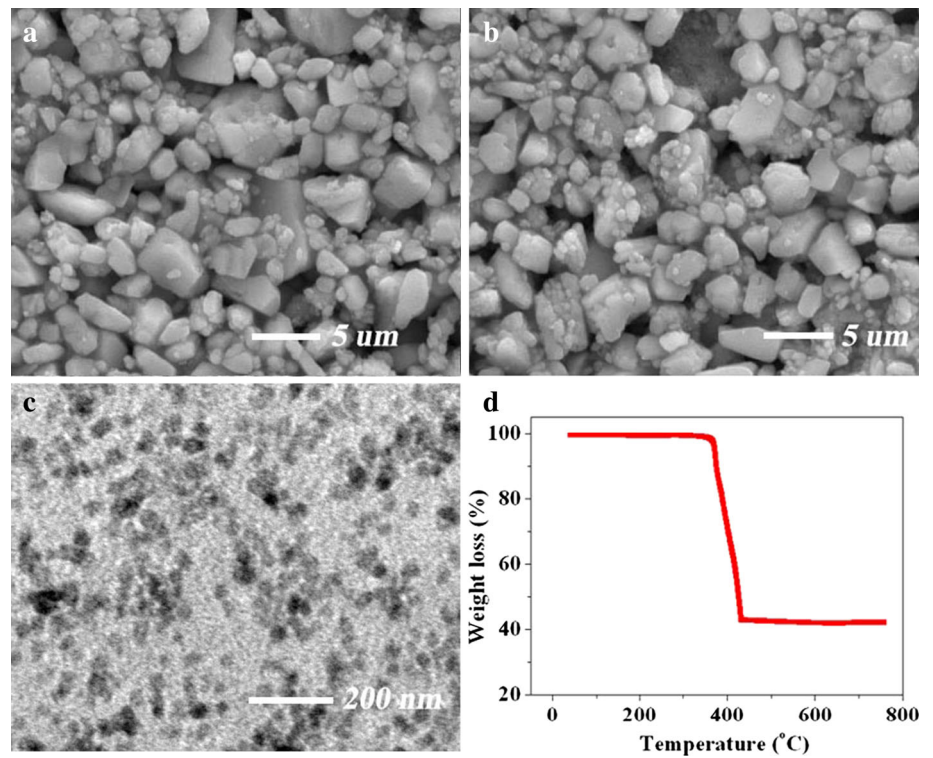
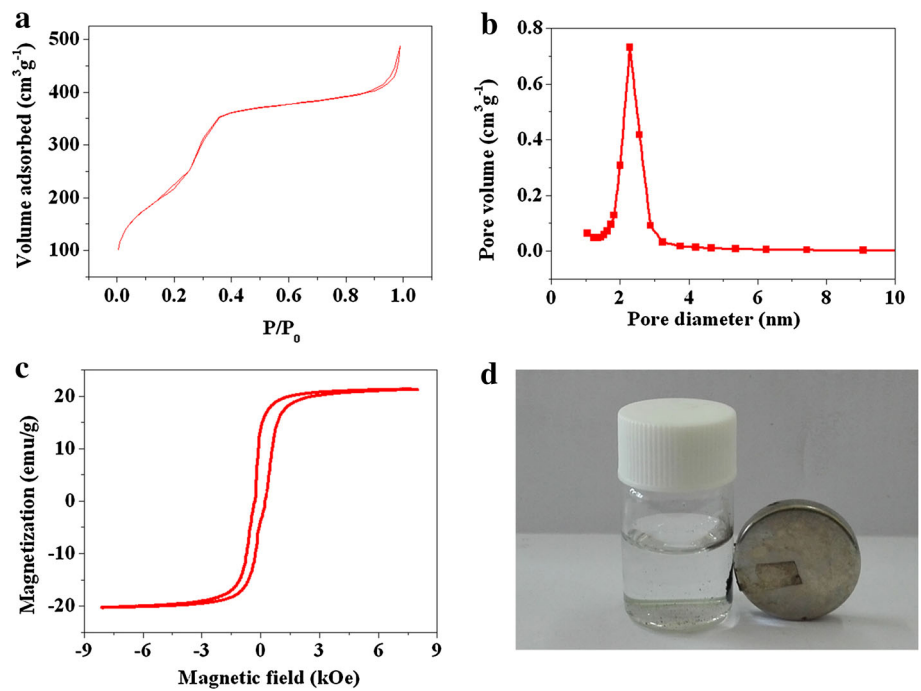


Fig. 4 **a** N₂ adsorption and desorption isotherms of Fe₃O₄/C at 77 K **b** pore size distribution of Fe₃O₄/C **c** magnetization curve of Fe₃O₄/C at room temperature **d** magnetization characteristic of Fe₃O₄/C

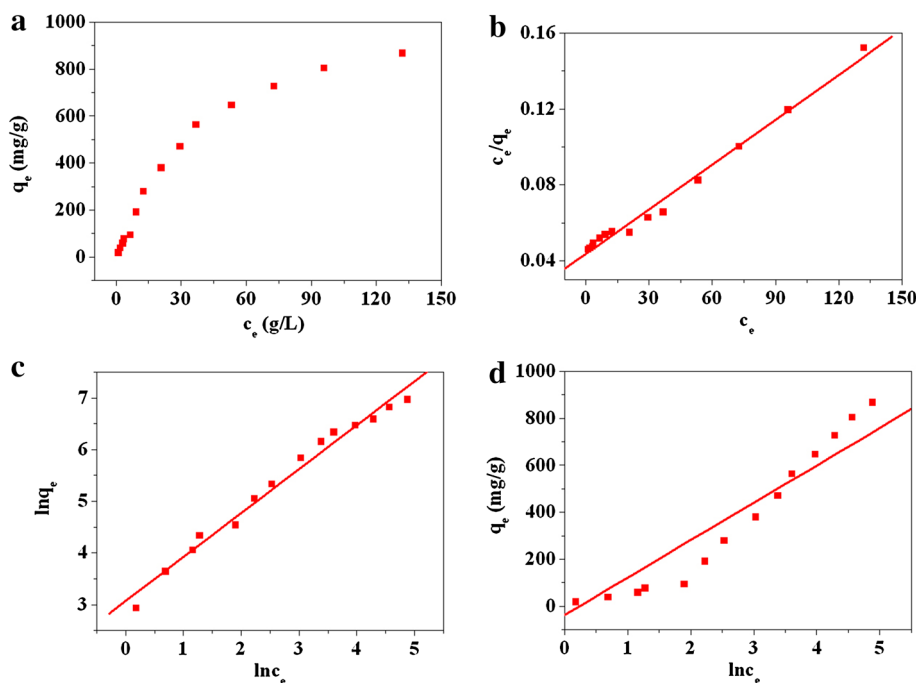


the adsorption behavior of ciprofloxacin on Fe₃O₄/C accurately. On the contrary, if the other two models are fitted, the results are worse than Langmuir model obviously (Fig. 5c, d). All these suggest ciprofloxacin is adsorbed of on surface of Fe₃O₄/C homogeneously.

3.4 Adsorption kinetics

In order to investigate the adsorption process of ciprofloxacin on Fe₃O₄/C, adsorption experiments were conducted with different initial concentrations (400, 600 and

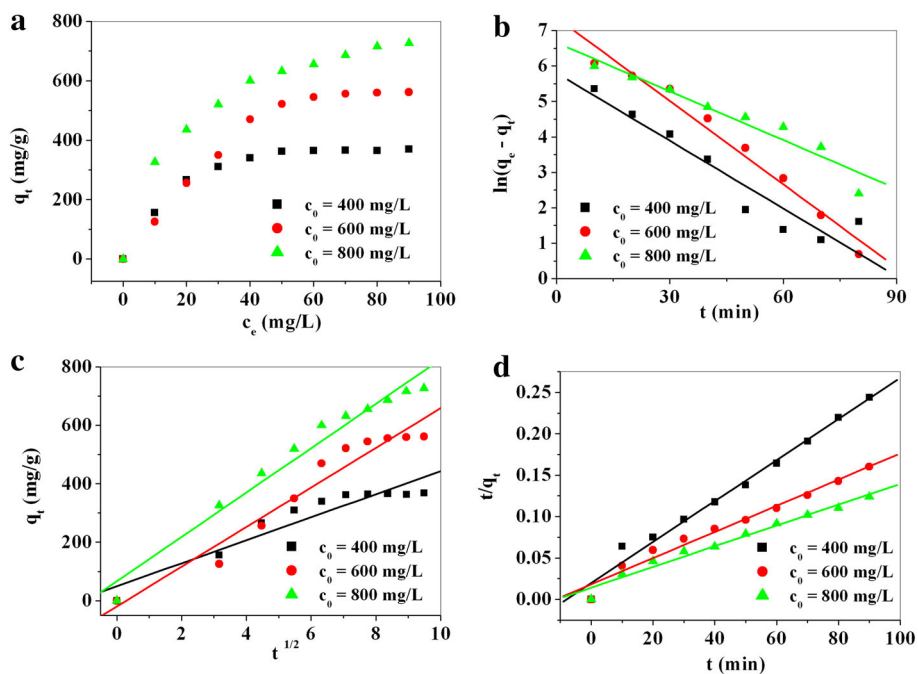
Fig. 5 **a** adsorption isotherm of $\text{Fe}_3\text{O}_4/\text{C}$ **b** Langmuir model fitting for the adsorption of ciprofloxacin by $\text{Fe}_3\text{O}_4/\text{C}$ **c** Freundlich model fitting for the adsorption of ciprofloxacin by $\text{Fe}_3\text{O}_4/\text{C}$ **d** Temkin model fitting for the adsorption of ciprofloxacin by $\text{Fe}_3\text{O}_4/\text{C}$



800 mg/L) and three kinds of kinetic models were used (Fig. 6a). According to the pseudo-first-order equation, the data does not show any linear relationships between $\ln(q_e - q_t)$ and adsorption time t , which verifies that the adsorption kinetic on $\text{Fe}_3\text{O}_4/\text{C}$ does not follow this model (Fig. 6b). If intra-particle diffusion model was tested, the same result was obtained (Fig. 6c). At last, pseudo-second-

order was applied to analyze the experimental data. It is found that all the correlation coefficients (R^2) of the linear form of pseudo-second-order model were 0.9961, 0.9925, and 0.9906, respectively (Fig. 6d). The calculated adsorption capacity (q_e) values estimated by the pseudo-second-order model are 355.05, 542.26, and 711.31 mg/g, which show good consistency with the detected values in

Fig. 6 **a** Adsorption capacity of ciprofloxacin versus time with different initial concentrations **b** pseudo-first-order model kinetics model for adsorption of ciprofloxacin by $\text{Fe}_3\text{O}_4/\text{C}$ **c** intra diffusion model kinetics model for adsorption of ciprofloxacin by $\text{Fe}_3\text{O}_4/\text{C}$ **d** pseudo-second-order model kinetics model for adsorption of ciprofloxacin by $\text{Fe}_3\text{O}_4/\text{C}$



experiment (369.43, 562.38, and 727.97, respectively). This indicated that the pseudo-second-order model is more suitable for the adsorption process of ciprofloxacin on Fe₃O₄/C.

3.5 Adsorption thermodynamics

To optimize the adsorption condition, three temperatures were designed to explore the thermodynamics of the adsorption of ciprofloxacin on Fe₃O₄/C (Fig. 7a). With the enhancement of temperature, the value of equilibrium constant also increases (K), which implies the adsorption is an endothermic process (Fig. 7b). To further study the thermodynamics, the calculation of thermodynamics parameters, such as ΔG, ΔH and ΔS is necessary (Table 1). In the test temperature range, all ΔG values are negative, which suggests the adsorption process is spontaneous. Furthermore, the most negative ΔG value is obtained at the highest temperature, which implies that higher temperature is more favorable. The positive ΔH value (25.68 kJ mol⁻¹) further proves the endothermic nature of the adsorption, which is in accordance with fact that higher temperature

results better adsorption effect. At last, the positive ΔS (0.127 kJ mol⁻¹ K⁻¹) value reflects an enhancement of randomness during the adsorption process. Based on these thermodynamics parameters, we can conclude, the treatment of ciprofloxacin containing waste water with Fe₃O₄/C should be conducted at higher temperature, while desorption process should be performed at lower temperature.

For a magnetic adsorbent as Fe₃O₄/C, repeatability is the most crucial factor for practical application. The repeatability of Fe₃O₄/C was studied with initial concentration of ciprofloxacin are 100 and 200 mg/L respectively (Fig. 7c, d). When adsorption was complete, Fe₃O₄/C was separated with magnetic separation technology with an external magnetic field and washed with ethanol. The magnetic separation technology not only simplifies the operation process, but also improves the recovery efficiency of adsorbent. The recovery efficiency of Fe₃O₄/C reaches 96 %, which is much higher than mesoporous carbon without Fe₃O₄ embedding in the framework (82 %). To study the renewability, ethanol solution (10 %) was used to eluted adsorbed ciprofloxacin on Fe₃O₄/C (initial concentration of ciprofloxacin was 200 mg/L).The result

Fig. 7 **a** Adsorption capacity of ciprofloxacin under different temperatures **b** thermodynamics analysis of ciprofloxacin adsorption process by Fe₃O₄/C **c** cycling runs of Fe₃O₄/C with initial ciprofloxacin concentration 100 mg/L **d** cycling runs of Fe₃O₄/C with initial ciprofloxacin concentration 200 mg/L

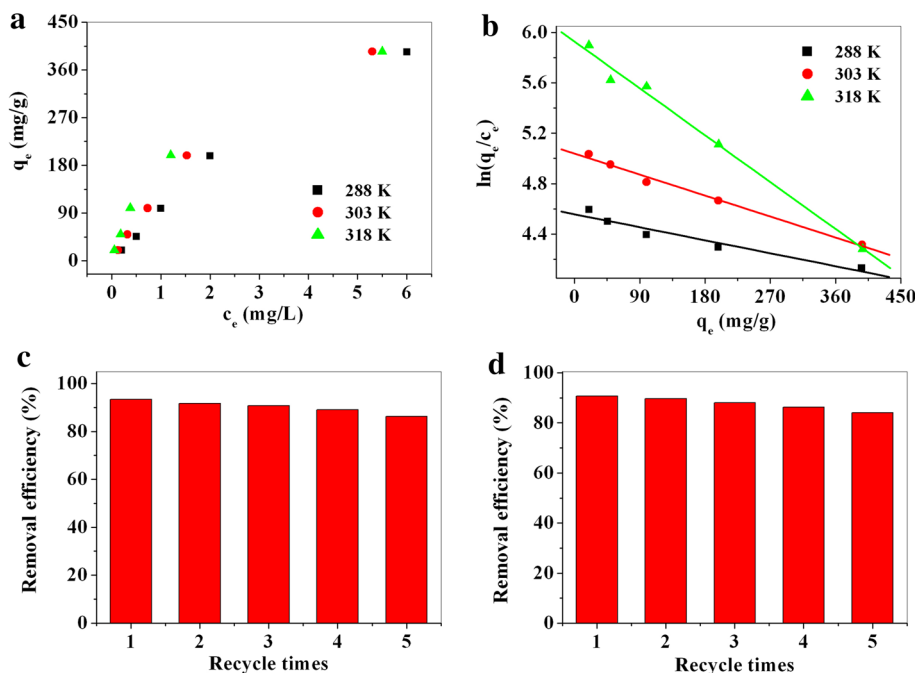


Table 1 Thermodynamics parameters of tetracycline adsorption process at different temperatures

T (K)	K ⁰	ΔG (kJ mol ⁻¹)	ΔH (kJ mol ⁻¹)	ΔS (kJ mol ⁻¹ K ⁻¹)
293	21.11	-51.42	65.51	0.362
308	17.96	-45.99		
323	12.02	-32.28		

illustrates elution efficiency reaches 86.5 %. After recycled for five times, its removal efficiency only decreases about 5 %, which indicates Fe₃O₄/C possesses favorable recycling property (Fig. 7b).

4 Conclusion

In this paper, magnetic mesoporous carbon material was synthesized successfully through the calcination of a mixed valence Fe based MOF precursor. The experimental results indicate that Fe₃O₄/C can effectively remove ciprofloxacin in aqueous solution. Although the removal rate decreases with the increasing of concentration, this value still reaches 93.9 % as concentration of ciprofloxacin is as high as 600 mg/L. The adsorption isotherm can be well fitted by the Langmuir adsorption isotherm equation with the maximum adsorption capacity of 868.6 mg/g. Kinetic studies suggest that the adsorption equilibrium follows pseudo-second-order model and can be achieved quickly. Furthermore, thermodynamic parameters imply the adsorption of ciprofloxacin on Fe₃O₄/C is a spontaneous, endothermic and entropy increasing process. In Fe₃O₄/C, Fe₃O₄ nanoparticle resides inside; this makes this adsorbent can be separated and recycled easily through with magnetic separation techniques. These results suggest that Fe₃O₄/C is a convenient and powerful adsorbent for the treatment of ciprofloxacin containing waste water.

Acknowledgments This work was supported by National Natural Science Foundation (21303010) and Fundamental Research Funds for the Central Universities (L1505003).

References

- M. Ferech, S. Coenen, S. Malhotra-Kumar, K. Dvorakova, E. Hendrickx, C. Suetens, H. Goossens, *J. Antimicrob. Chemother.* **58**, 423 (2006)
- H.A. Duong, N.H. Pham, H.T. Nguyen, T.T. Hoang, H.V. Pham, V.C. Pham, M. Berg, W. Giger, A.C. Alder, *Chemosphere* **72**, 968 (2008)
- N. Adriaenssens, S. Coenen, A. Versporten, A. Muller, G. Minalu, C. Faes, V. Vankerckhoven, M. Aerts, N. Hens, G. Molenberghs, H. Goossens, *J. Antimicrob. Chemother.* **66**, 47 (2011)
- A. Speltini, M. Sturini, F. Maraschi, A. Profumo, *J. Sep. Sci.* **33**, 1115 (2010)
- A.K. Sarmah, M.T. Meyer, A.B.A. Boxall, *Chemosphere* **65**, 725 (2006)
- A.C. Martins, O. Pezoti, A.L. Cazetta, K.C. Bedin, D.A.S. Yamazaki, G.F.G. Bandoch, T. Asefa, J.V. Visentainer, V.C. Almeida, *Chem. Eng. J.* **260**, 291 (2015)
- Y. Gao, Y. Li, L. Zhang, H. Huang, J.J. Hua, S.M. Shah, X.G. Su, *J. Colloid. Interface Sci.* **368**, 540 (2012)
- H. Wang, N. Yan, Y. Li, X.H. Zhou, J. Chen, B.X. Yu, M. Gong, Q.W. Chen, *J. Mater. Chem.* **22**, 9230 (2012)
- L.C.A. Oliveir, R.V.R.A. Rios, J.D. Fabris, V. Garg, K. Sapag, R.M. Lago, *Carbon* **40**, 2177 (2002)
- L.Q. Ji, L.C. Zhou, X. Bai, Y.M. Shao, G.H. Zhao, Y.H. Qu, C. Wang, Y.F. Li, *J. Mater. Chem.* **22**, 15853 (2012)
- T. Ren, Y. Si, J.M. Yang, B. Ding, X.X. Yang, F. Hong, J.Y. Yu, *J. Mater. Chem.* **22**, 15919 (2012)
- W. Fan, W. Gao, C. Zhang, W.W. Tjiu, J.S. Pan, T.X. Liu, *J. Mater. Chem.* **22**, 25108 (2012)
- W.M. Xuan, C.F. Zhu, Y. Liu, Y. Cui, *Chem. Soc. Rev.* **41**, 1677 (2012)
- S.L. Li, Q. Xu, *Energy Environ. Sci.* **6**, 1656 (2013)
- X.L. Yan, X.J. Li, Z.F. Yan, *Appl. Surf. Sci.* **308**, 306 (2014)
- Z.X. Zhong, J.F. Yao, Z.X. Low, R.Z. Chen, M. He, H.T. Wang, *Carbon* **72**, 242 (2014)
- S. Lim, K. Suh, Y. Kim, M. Yoon, H. Park, D.N. Dybtsev, K. Kim, *Chem. Commun.* **48**, 7447 (2012)
- F.H. Bai, Y.D. Xia, B.L. Chen, H.Q. Su, Y.Q. Zhu, *Carbon* **79**, 213 (2014)
- S. Zhong, C.X. Zhan, D.P. Cao, *Carbon* **85**, 51 (2015)
- A.J. Amali, J.K. Sun, Q. Xu, *Chem. Commun.* **50**, 1519 (2014)
- R.W. Liang, F.F. Jing, L.J. Shen, N. Qin, L. Wu, *J. Hazard. Mater.* **287**, 364 (2015)
- C. Raji, T.S. Anirudhan, *Water Res.* **32**, 3772 (1998)
- P. Horcajada, C. Serre, G. Maurin, N.A. Ramsahye, F. Balas, M. Vallet-Regí, M. Sebban, F. Taulelle, G. Férey, *J. Am. Chem. Soc.* **130**, 6774 (2008)
- W. Cheng, K.B. Tang, Y.X. Qi, J. Sheng, Z.P. Liu, *J. Mater. Chem.* **20**, 1799 (2010)
- C. Petit, J. Burrell, T.J. Bandosz, *Carbon* **49**, 563 (2011)
- K. Cheng, Y.M. Zhou, Z.Y. Sun, H.B. Hu, H. Zhong, X.K. Kong, Q.W. Chen, *Dalton Trans.* **41**, 5854 (2012)
- S. Qu, F. Huang, S.N. Yu, G. Chen, J.L. Kong, *J. Hazard. Mater.* **160**, 643 (2008)
- E. Kim, M. Koon, *J. Porous Mater.* **22**, 1495 (2015)
- D.W. Wang, F. Li, G.Q. Lu, H.M. Cheng, *Carbon* **46**, 1593 (2008)